Journal of Fluids and Structures 18 (2003) 367–386

JOURNAL OF FLUIDS AND STRUCTURES

www.elsevier.nl/locate/jnlabr/yjfls

The effect of flow perturbations on the near wake characteristics of a circular cylinder

E. Konstantinidis, S. Balabani, M. Yianneskis*

Experimental and Computational Laboratory for the Analysis of Turbulence (ECLAT), Department of Mechanical Engineering, King's College London, Strand, London WC2R 2LS, UK

Received 21 October 2002; accepted 11 July 2003

Abstract

The mean and fluctuating velocity fields in the near wake of a circular cylinder subjected to an incident mean flow with periodic velocity perturbations superimposed upon it were examined using laser Doppler anemometry. From these measurements the wake was characterized in terms of the recirculation bubble length, vortex formation length, maximum intensity of the velocity fluctuations and the wavelength of the vortex street. The well-known 'lock-on' phenomenon was observed for perturbation frequencies around two times the natural vortex shedding frequency. It is shown that the wake structure is modified in a systematic manner within the lock-on range. The forced wake shares many basic characteristics as that of a cylinder oscillating either transversely or in line, relative to the flow direction. These include the shortening of the recirculation bubble and the vortex formation region as well as the variation of the longitudinal vortex spacing with perturbation frequency. Differences but also similarities between forced wakes at low (less than 350) and relatively higher Reynolds numbers (greater than 350) are discussed.

1. Introduction

The phenomenon of vortex shedding lock-on due to either forced or self-induced cylinder oscillations in crossflow has been extensively studied over the past decades, e.g., see the review papers by Sarpkaya (1979), Bearman (1984) and Griffin and Hall (1991). The problem continues to attract considerable interest as evidenced by a number of recent studies, for example, see Carberry et al. (2001), Govardhan and Williamson (2001) and Krishnamoorthy et al. (2001). The majority of previous studies have concentrated upon transverse oscillations of the cylinder since the fluctuating lift is the dominant force. However, lock-on or synchronization of the wake and oscillation frequencies can also take place when a cylinder oscillates in line with the incident flow (Griffin and Ramberg, 1976; Ongoren and Rockwell, 1988). Similarly, lock-on can also be observed when the cylinder is stationary and the incident mean flow has a periodic component superimposed upon it (Barbi et al., 1986; Armstrong et al., 1986; Hall and Griffin, 1993). This type of flow, termed perturbed flow here, is equivalent to in-line oscillations of the cylinder in a steady incident flow when the perturbation wavelength is large compared to the cylinder diameter (Griffin and Hall, 1991). There is typically a range of perturbation frequencies, f_e, around twice the natural Strouhal frequency in the unforced (unperturbed) wake, f_o, where the vortex shedding frequency, f_s, remains locked-on to precisely half the perturbation frequency, i.e., $f_s = f_e/2$ when $f_e/f_o \approx 2$; this range constitutes the fundamental lock-on regime in analogy to the fundamental lock-on regime from a cylinder oscillating transversely in a steady flow which occurs for frequency ratios around unity. The perturbation frequency need be close to twice the shedding frequency to capture the wake frequency because the

*Corresponding author. Tel.: +44-20-7848-2428; fax: +44-20-7848-2932.
E-mail address: michael.yianneskis@kcl.ac.uk (M. Yianneskis).

0889-9746/$ - see front matter
doi:10.1016/j.jfluidstructs.2003.07.006

fluctuations in the drag force, i.e., in the direction of the perturbation, occur at twice the nominal shedding frequency due to the fact that each of the two alternating vortices that are shed during a cycle independently induces a fluctuating component. The range of frequency ratios, f_e/f_o, over which lock-on occurs increases as the perturbation amplitude increases and is Reynolds number dependent (Griffin and Hall, 1991). Moreover, additional lock-on states might also be possible at $f_e/f_o \approx 3$ and 4 as in the case of equivalent in-line cylinder oscillations (Ongoren and Rockwell, 1988).

Related studies show that the fundamental lock-on is accompanied by a number of changes in the resulting forces on the body and the wake structure. Barbi et al. (1986) found that the magnitude of the mean drag and the fluctuating lift forces increased at lock-on compared to those in the unperturbed flow. Their findings agree well with the early experiments of Tanida et al. (1973), who found that the mean drag and fluctuating lift forces on a cylinder oscillating in line with the incident flow attain maximum values near the middle of the lock-on range, i.e., when the frequency of the oscillations was nearly twice the unforced Strouhal frequency. The above effects are associated with modification of the near wake structure behind the cylinder. Armstrong et al. (1987) found that, in the middle of the lock-on range, the strength of the shed vortices increased by 29% and the vortex formation length decreased from 1.2 to 0.9 cylinder diameters compared to that in the unperturbed flow. The latter result disagrees with the numerical simulations of Hall and Griffin (1993) of a perturbed flow wake at $\mathrm{Re} = 200$, which predict an expansion of the vortex formation length. This contradiction might be attributed to the different mechanics of vortex formation and shedding at low Reynolds numbers (less than $\mathrm{Re} = 350$) to that at relatively higher Reynolds numbers (greater than $\mathrm{Re} = 350$) as described in Gerrard (1966) and Green and Gerrard (1993) and discussed further in Griffin (1995). The above suggest that flow perturbations or equivalent cylinder oscillations can have varying effects depending on the Reynolds number. Griffin and Ramberg (1976) found that the wavelength of the vortex street varies inversely with the frequency of an oscillating cylinder in line with the incident flow within the lock-on range and there is evidence from the computations of Hall and Griffin (1993) that the perturbed flow wake exhibits the same behavior.

The near wake structure behind a bluff body plays an important role in the overall vortex formation and shedding processes and determines the magnitude of the mean and fluctuating forces exerted on the body. Its experimental study, however, is difficult due to the prevailing flow conditions which include regions of pronounced reversed flow and high-turbulence levels, particularly at high Reynolds numbers. Available data on the mean velocity field exhibit considerable sensitivity on the experimental conditions (Ma et al., 2000). Accurate and reliable experimental data are required in order to improve understanding of vortex shedding lock-on phenomena and for testing and validation of numerical simulations of the flow around stationary and vibrating bluff bodies which are of great importance in engineering structures such as heat exchangers, offshore platforms, power cables, etc. In many of these applications, the incident mean flow contains periodic perturbations superimposed upon it, e.g. when a body is placed in the wake of another one, in flows delivered by reciprocating pumps, structures under the influence of combined current—waves, etc.

This paper describes a systematic study of the effects of velocity perturbations superimposed upon the incident mean flow on the near wake characteristics of a circular cylinder as the reduced velocity $U^* = U/f_e d$, where f_e is the perturbation frequency, d the cylinder diameter and U the mean approach velocity, spans the lock-on range, i.e., $U^* = 2.1$–2.9 (equivalent to frequency ratios $f_e/f_o = 1.6$–2.3). In the present study, lock-on is achieved by varying the perturbation frequency. The Reynolds number ($\mathrm{Re} = Ud/\nu$) is in the range 10^3–10^4 (high Re mode) for which limited data exist; however, the perturbed flow experiments were undertaken at a Reynolds number of 2150, based on the mean approach velocity. The dimensionless amplitude $\varepsilon = \Delta u/(2\pi f_e d)$, where Δu is the amplitude of the flow perturbations, which is equivalent to the ratio of the amplitude of an oscillating cylinder to its diameter, ranges from 0–0.1 (velocity ratios $\Delta u/U$ in the range 0–0.2). Laser Doppler anemometry (LDA), which is noninvasive and particularly suited for the prevailing flow conditions, is employed to measure the instantaneous velocity fluctuations in the near wake and ascertain the flow field in terms of mean velocity, r.m.s. fluctuation and spectral content. The paper focuses on the variation of the extent of the recirculation bubble and the vortex formation region, the change in the longitudinal vortex spacing and the modification of the wake structure within the lock-on range.

2. Experimental apparatus and procedures

The experiments were conducted in a stainless-steel water tunnel facility which consists of a closed-circuit flow installation equipped with a 9:1 contraction and appropriate arrangements of hexagonal honeycomb and screens to condition the flow approaching the 72 mm × 72 mm working section. The working section was made of transparent Plexiglas to allow optical access for LDA measurements and flow visualization. The streamwise turbulence level measured in the empty working section with the laser anemometer was 3.3% and the velocity variation in the core flow was less than 0.5% outside the wall boundary layers. The facility included temperature control of the working fluid via a double-jacketed collection tank and an external cooling/heating unit. A centrifugal pump provided the bulk flow in

the tunnel and a bypass adjusted the average flowrate, which was monitored with a magnetic flowmeter. Velocity perturbations superimposed on the mean approach flow were introduced via the action of a rotating valve driven by a variable speed motor. The rotating valve periodically blocked the passage of part of the flow thereby inducing nearly sinusoidal velocity perturbations (see Fig. 1). The torque of the motor was sufficiently high to ensure that the rotational frequency of the valve was constant within ± 0.05 Hz and, hence, no feedback control was necessary. The perturbation frequency was adjusted in the range 14.6–20.0 Hz via a knob on the motor supply unit and monitored with a digital frequency meter, which was fed with the pulses from an optical encoder attached to the shaft of the rotating valve. The relative amounts of perturbed/unperturbed flow were adjusted by control valves, which in effect provided a means of controlling the amplitude of the perturbations independently of the frequency and mean approach velocity. The perturbation amplitude was deduced by phase averaging the fluctuating velocity signal at the reference point, located 22 mm upstream of the test cylinder (see Fig. 1). A similar configuration for the generation of flow perturbations was previously used in a similar water tunnel and an assessment of the perturbation characteristics can be found in Konstantinidis (2001).

The experiments reported in this paper were carried out with a smooth Plexiglas circular cylinder, 7.2 mm in diameter, unless otherwise stated. The cylinder spanned the entire working section and was rigidly mounted on the section walls in order to eliminate the possibility of vibrations, which would interfere with the measurements being taken. Velocity measurements obtained at different spanwise stations showed that both the time-mean statistics (up to the fourth order) and the spectral characteristics were sufficiently similar along the span of the cylinder, indicating thus a nominally two-dimensional (2-D) flow. It should be noted, however, that in the Re range tested the instantaneous wake flow is strongly three dimensional.

A three-probe four-component LDA system (Dantec™) was employed for the velocity measurements in the near wake of the cylinder. The system consisted of a 5 W argon-ion laser, two transmitter boxes for separation of the laser light into three colors (green, blue and violet) equipped with Bragg cells for frequency shifting, three probes with built-in collection optics and optical fibers for transmitting and receiving the laser light. The light received by the collection optics was separated by color separators and fed to four individual photomultipliers. The signal from the photomultipliers was processed with four burst spectrum analysers (BSAs) interfaced to a personal computer with appropriate hardware and software for data acquisition. The velocity samples from each BSA were registered with reference to a common clock source. For the majority of the present measurements, a 2-D probe measuring two perpendicular velocity components was mounted on an automated transverse table to scan the wake flow and a single-component probe (1-D) was mounted on a manual transverse table to monitor the flow conditions at a reference point, located 22 mm upstream of the test cylinder. The dimensions of the measuring control volumes are shown in Table 1.

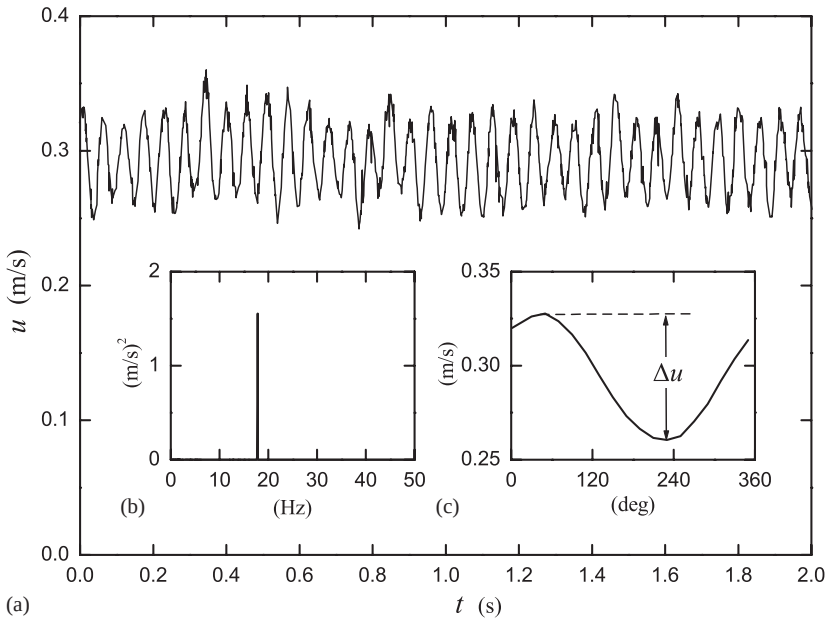

Fig. 1. Instantaneous velocity perturbations upstream of the test cylinder (a), spectrum of the fluctuating velocity (b) and waveform of the perturbations resulting from averaging the velocity signal at constant phase (c) for a typical case.

Table 1
Dimensions of the measuring control volume (mm)

Probe	x	y	z	Component
1-D	0.116	0.115	1.646	u
2-D	0.078	0.077	0.677	u
2-D	0.074	0.073	0.633	v

The LDA technique inherently yields individual data randomly distributed in time as particles suspended in the fluid pass through the measuring control volume. As a result, estimation of the mean and root mean square (r.m.s.) velocities as well as spectra requires special attention since the simple arithmetic operations applied on uniformly distributed data, e.g., such as those from hot-wire anemometry, are not applicable and may lead to considerable errors. In this study, ensemble-averaged mean and r.m.s. velocities were computed, respectively, using the weighted averages

$$\bar{u} = \frac{\sum_i w_i u_i}{\sum_i w_i} \tag{1}$$

and

$$u' = (u_i^2)^{0.5} = \left[\frac{\sum_i w_i (u_i - \bar{u})^2}{\sum_i w_i}\right]^{0.5}, \tag{2}$$

where the transit time of the particles through the measuring control volume was employed as a weighting factor to eliminate velocity bias (Buchhave et al., 1979). The correction procedure proposed by Durst et al. (1995) to take into account the finite size of the measuring control volume yielded negligible errors when applied to the present data and therefore was not implemented. Furthermore, nonturbulent broadening of the Doppler frequency due to other sources was estimated to be negligible (e.g., see Durst et al., 1976). In order to estimate spectra of the fluctuating velocities, the acquired raw nonequally spaced LDA data were resampled at equally spaced time intervals using a zero-order interpolation technique ('nearest neighbor'). The spectra were subsequently computed using fast Fourier transform methods. The resampling rate employed was always less than the average raw data rate. The latter was dependent on the mean approach velocity and measurement location (in general, the data rate is proportional to the local mean velocity). For the majority of the measurements reported here, the data rate was above 500 samples/s, which is sufficiently high to resolve both the low-frequency fluctuations associated with organized flow due to periodic vortex shedding and most of the high-frequency turbulent fluctuations.

The experimental uncertainties for the mean and r.m.s. velocities were determined by taking into account all sources of error and the repeatability was established from several repeats of the same experiment. The maximum uncertainties were as follows: $\bar{u} = \pm 5\%$, $u' = \pm 10\%$ and $v' = \pm 10\%$. It should be noted that the measurement error of the individual velocity samples is approximately 1%. The uncertainties reported above take into account the statistical error due to the finite number of samples acquired and the effect of velocity bias on the results.

3. Wake characteristics in unperturbed flow

A preliminary study of the wake in unperturbed (steady) flow was undertaken initially for providing a basis for comparisons. LDA measurements of the streamwise and transverse velocity components were carried out along the center-line of the cylinder wake and the results, obtained at four different Reynolds numbers, are shown in Figs. 2–4. The origin of the coordinate system employed is at the center of the circular cylinder; x and y are the streamwise and transverse directions, respectively.

Fig. 2 shows the distribution of the streamwise mean velocity, $\bar{u}$, normalized with the mean approach velocity, U, along the wake center-line. A region of reversed flow (negative mean velocities) exists near the base of the cylinder which defines the recirculation bubble. The velocity reaches a minimum (maximum negative) value adjacent to the cylinder and then increases sharply to positive values followed by an asymptotic trend further downstream. The position downstream of the cylinder where the mean velocity becomes zero is a characteristic length scale of the wake, referred to as the recirculation bubble length (l_b). Comparison of l_b values measured for steady flow in the present study with other published data is made later in Fig. 5. At $x/d = 8$ the mean velocity has recovered to about 80% of the mean approach velocity.

The distribution of the normalized streamwise r.m.s. velocity, u'/U, along the wake center-line is shown in Fig. 3(a). It displays a characteristic peak the position of which is a measure of the so-called vortex formation length (Griffin,

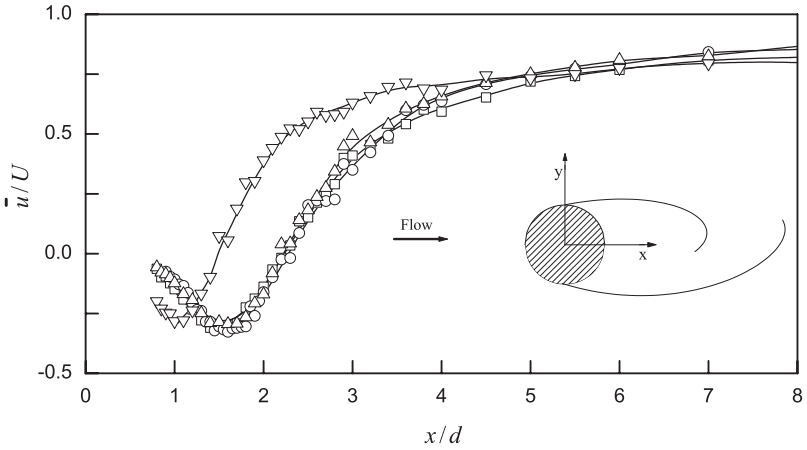

Fig. 2. Distribution of the streamwise mean velocity along the wake center-line for four different Reynolds numbers: □, Re = 1550; ○, Re = 2150; △, Re = 2750; ▽, Re = 7450.

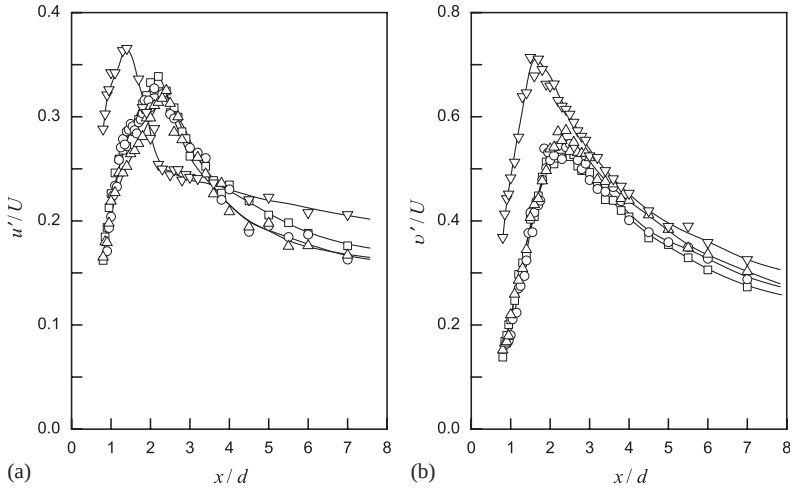

Fig. 3. Distribution of the (a) streamwise and (b) transverse r.m.s. velocities along the wake center-line for four different Reynolds numbers: □, Re = 1550; ○, Re = 2150; △, Re = 2750; ▽, Re = 7450.

1995). A similar peak is observed for the distribution of transverse r.m.s. velocity (Fig. 3(b)). The magnitude of the transverse fluctuations is roughly two times that of the streamwise component at all positions due to the way that vortices are formed, typical of many bluff body wakes.

The maximum r.m.s. fluctuations measured along the wake center-line in the present study are compared with other values reported in the literature in Table 2. The maximum streamwise r.m.s. velocities, u'/U_{max}, appear slightly higher compared to the other reported values but only marginally; however, the maximum transverse r.m.s. velocities, $(v'/U)_{max}$, are noticeably higher. This might be attributed to the relatively high-turbulence levels of the approach flow (3.3%) and the relatively high blockage from the cylinder (10–14%). High-turbulence levels promote turbulent transition in the separating shear layers close to the cylinder and result in increased entrainment of free stream fluid into the near wake whereas, the relatively high blockage is known to intensify the velocity fluctuations in the wake. These effects due to turbulence and blockage tie in with the abrupt shortening of the recirculation bubble at the higher Reynolds numbers tested, as discussed below.

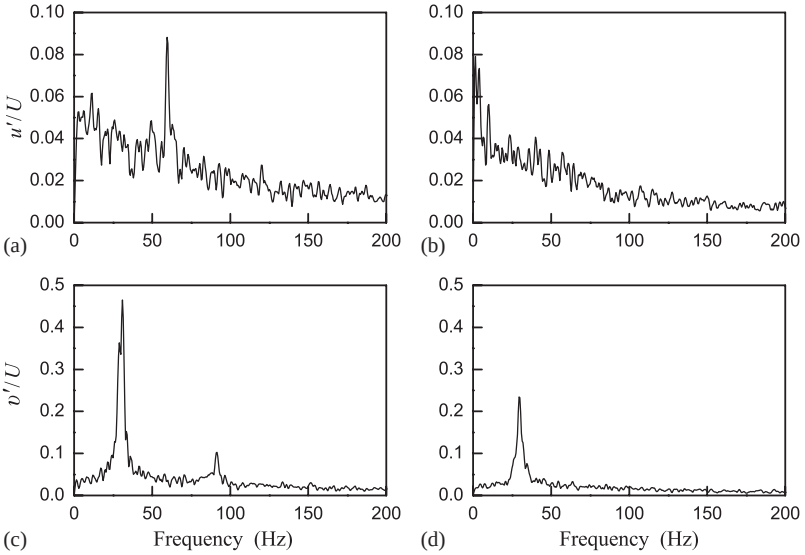

Fig. 4. Spectra of the velocity fluctuations in the wake center-line for Re = 7450; (a) u spectrum, $x/d = 3.2$, (b) u spectrum, $x/d = 10$, (c) v spectrum, $xld = 3.2$ and (d) v spectrum, $x/d = 10$. Vortex shedding frequency: $f_0 = 30$ Hz. The resolution of the spectrum is 0.5 Hz.

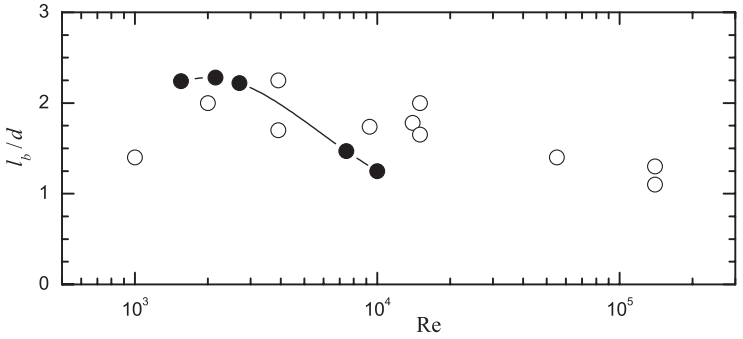

Fig. 5. Variation of the recirculation bubble length with Reynolds number in unperturbed flow: •, present data; ○, compilation of data reported in McKillop and Durst (1984), Ma et al. (2000) and Govardhan and Williamson (2001).

Table 2
Peak r.m.s. fluctuation along the wake center-line of a circular cylinder

Study	Re	$(u'/U)_{max}$	$(v'/U)_{max}$
Present	1550	0.33	0.53
Present	2150	0.32	0.54
Present	2750	0.31	0.56
Norberg (1986)	3000	0.28	—
Govardhan and Williamson (2001)	3900	0.22	0.48
Present	7450	0.35	0.69
Norberg (1986)	8000	0.30	—
Present	10^4	0.39	0.80
Cantwell and Coles (1986)	1.4×10^5	0.47	0.66

Fig. 4 shows spectra of both u and v fluctuations at two axial locations in the wake center-line. The u spectra display a distinct periodicity at twice the vortex shedding frequency (60 Hz), whereas the v spectra at the same location display a pronounced periodicity at the shedding frequency and a weaker one at the third harmonic of it. It should be noted that

the scale for the v spectra in Figs. 4(c) and (d) is five times that of the u spectra in Figs. 4(a) and (b). Clearly, the periodicity detected in the spectra is associated with the vortex formation and shedding processes. As vortices form alternately on both sides of the cylinder, they cause a fluctuating velocity field. On the wake center-line the u component oscillates at twice the shedding frequency due to the influence of the vortices on either side of the center-line. Further downstream at $x/d = 10$, the periodicity is hardly detected in the u spectra and becomes less pronounced in the v spectra owing to the decay of the strength of the vortices and their disintegration. The magnitude of the peaks in the spectra indicates that most of the energy of the v fluctuations is mainly due to the organized flow associated with vortex shedding, whereas organized flow and turbulence contribute approximately equally to the energy of the u fluctuations.

Fig. 5 shows a compilation of data from the present and previously published studies that illustrates the variation of the recirculation bubble length, l_b, defined by the position of zero mean velocity along the wake center-line, as a function of Re. Values are normalized with the cylinder diameter to facilitate comparisons. Note that the value at $\mathrm{Re} = 10^4$ was obtained with a cylinder 10 mm in diameter. The present data appear to agree with published data for Re less than 3000 (by extrapolating the published data), but l_b appears to be shorter for the higher Re notwithstanding any experimental uncertainty in the data. The abrupt shortening of the recirculation bubble with increasing Reynolds number in the present study might be partially attributed to the relatively high tunnel blockage and partially to the relatively high-turbulence level of the incident flow. It is known that upstream turbulence can promote transition in the separating shear layers which roll up closer to the cylinder and is associated with a decrease in the length of the vortex formation region and of the recirculation bubble compared to that in a nominally smooth flow. Furthermore, the blockage from the cylinder is expected to be associated with a shorter recirculation bubble compared to a nominally unconfined flow.

The variation of the vortex formation length, l_f, defined by the position of the maximum streamwise r.m.s. fluctuation along the center-line, as a function of Re is shown in Fig. 6. The family of curved lines indicates the end of the formation region from Bloor's experiments (Bloor and Gerrard, 1966). Each curve corresponds to results obtained with different diameter cylinders and therefore represents the dependency of the vortex formation length on cylinder diameter. The present data show that the formation length increases marginally between $\mathrm{Re} = 1550$ and 2150 and then decreases to $1.1d$ at $\mathrm{Re} = 10^4$ (the latter value obtained with a 10 mm diameter cylinder). The present data (solid symbols) agree well with Bloor's data for the smallest cylinder (lower curve). The abrupt shortening of the vortex formation length between $\mathrm{Re} = 10^3 - 10^4$ has also been observed in low-turbulence water tunnel experiments (Unal and Rockwell, 1988; Lin et al., 1995). Norberg (1986) found that increasing the turbulence level from 0.1% to 1.4% resulted in only a slight upstream displacement of the position of the maximum r.m.s. fluctuation at both $\mathrm{Re} = 3000$ and 8000. This suggests that the effect of turbulence level alone on the vortex formation length is small. It is also known that the Strouhal number remains unaffected by turbulence in this Re range (Zdravkovich, 1997). However, the influence of aspect ratio, tunnel blockage, end effects, etc., appears to be important as evidenced by the scatter in the published data. The turbulence length scale might also be expected to have an effect on the vortex formation length. It should be noted, however, that the overlap of the present data obtained with different cylinder diameters in Figs. 4 and 5 (7.2 and 10 mm corresponding to $\mathrm{Re} = 7450$ and 10000, respectively), indicates that the combined effect of aspect ratio and blockage is not significant.

The position of maximum r.m.s. fluctuation in the transverse direction along the wake center-line is also shown in Fig. 6. Its variation is similar to that of l_f, although no direct correspondence can be found. The position of $(v'/U)_{\max}$ occurs slightly downstream of $(u'/U)_{\max}$ at all Reynolds numbers in the unperturbed flow. It might be argued that data

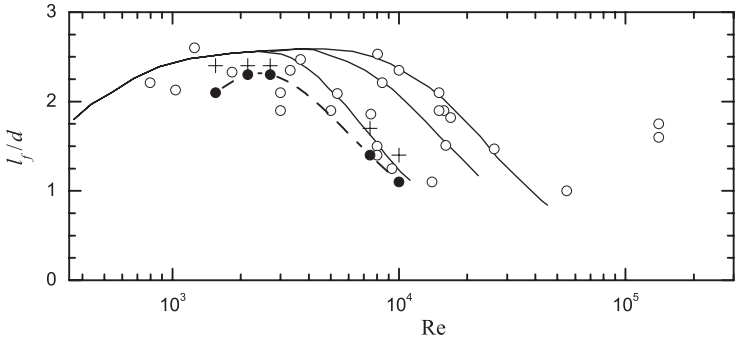

Fig. 6. Variation of the vortex formation length as a function of the Reynolds number in unperturbed flow. - - ● - -, present data; —— Bloor (1964); ○, compilation of data reported in Norberg (1986), McKillop and Durst (1984), Govardhan and Williamson (2001) and Krishnamoorthy et al. (2001); +, position of maximum transverse fluctuations in the present experiments.

obtained with a single stationary hot-wire probe are affected by the strong flow across the wake center-line, which causes the probe to be periodically immersed in irrotational fluid at wide angles. Therefore, the maximum r.m.s. fluctuation detected with a hot-wire probe might be expected to lie between the position of maximum r.m.s. fluctuation of the streamwise and transverse components. By taking this into consideration, the agreement between the present and published data is expected to be even better than that shown in Fig. 6.

4. The effect of flow perturbations

The effect of periodic velocity perturbations superimposed upon the mean approach flow on the wake characteristics was studied by LDA measurements along the center-line, similar to those described in the previous section for the unperturbed flow. All perturbed flow measurements were obtained at a constant approach velocity of $U = 0.30\,\mathrm{m\,s^{-1}}$ (Re = 2150) for which the recirculation bubble and the vortex formation region were relatively long.

4.1. Velocity spectra and fundamental lock-on range

The purpose of the present study is to examine the effect of flow perturbations on the wake characteristics within the fundamental lock-on range, i.e., the range of perturbation frequencies for which the vortex shedding frequency occurs at half the imposed perturbation frequency. One of the primary concerns is therefore to delineate the lock-on range. Based on preliminary tests carried out, a set of experimental conditions was selected, based on the limits of the experimental apparatus, to conduct the detailed investigation. Measurements were made while keeping the flow velocity and perturbation amplitude constant to $U = 0.30\,\mathrm{m\,s^{-1}}$ and $\Delta u = 0.03\,\mathrm{m\,s^{-1}}$, respectively, and varying the perturbation frequency, f_e, in the range 14.6–20.0 Hz.

Fig. 7 shows spectra of the transverse velocity fluctuations at a point in the wake center-line for perturbation frequencies around two times the natural shedding frequency (f_o). For $f_e/f_o = 1.63$ and 2.25 there is a modulation of the wake frequency by the imposed perturbations and the spectra display a broad-band peak around the natural vortex shedding frequency plus other peaks. Clearly, there is a transition from a modulated to a synchronized wake for perturbation frequencies closer to the resonant point $f_e/f_o = 2$. The frequency of the synchronized wake is exactly half

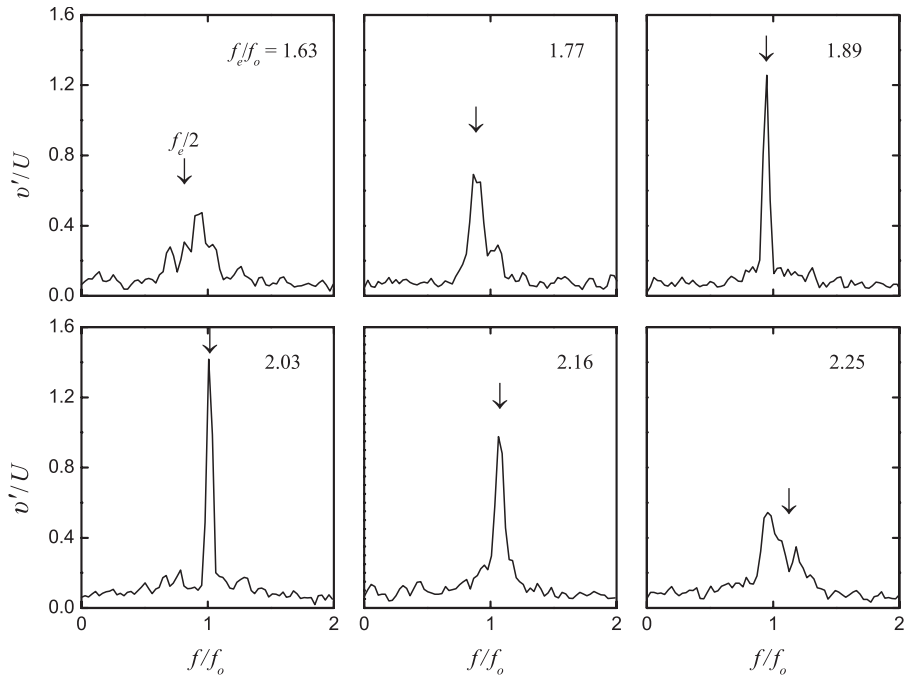

Fig. 7. Velocity spectra of the transverse velocity fluctuations at $x/d = 1.75$ in the wake center-line for different perturbation frequencies; $U = 0.30\,\mathrm{m\,s^{-1}}$; $\Delta u = 0.02\,\mathrm{m\,s^{-1}}$.

the perturbation frequency and the spectra display well-defined narrow-band peaks at this frequency, thus lock-on has taken place. The amplitude of the periodic velocity fluctuations in the wake associated with vortex shedding is considerably higher near the middle of the lock-on range.

Fig. 8 shows the variation of the vortex shedding frequency, f_s, as a function of the perturbation frequency, f_e. Values have been normalized with the natural shedding frequency, f_o, which is estimated from the constant Strouhal number relationship for the unperturbed flow, i.e., $f_o = 0.215U/d$. The shedding frequency was taken from the location of the highest peak in a number of spectra. There appears to be a gradual transition between locked-on and nonlocked-on states and therefore a quantitative criterion was used to define lock-on. The criterion employed here is that $0.99 < f_s/2f_e < 1.01$ to take into account the experimental uncertainty of the data. It should be noted that the nature of the lock-on states is rather statistical in the present experiments, meaning that the wake remains locked-on with the perturbations for most of the time but there might be deviations from this behavior as intermittent nonlocked-on intervals were also observed.

It is interesting to consider the simultaneous streamwise and transverse velocity fluctuations at a point in the wake center-line as shown in Fig. 9. Whereas the transverse velocity component shows periodic fluctuations with high

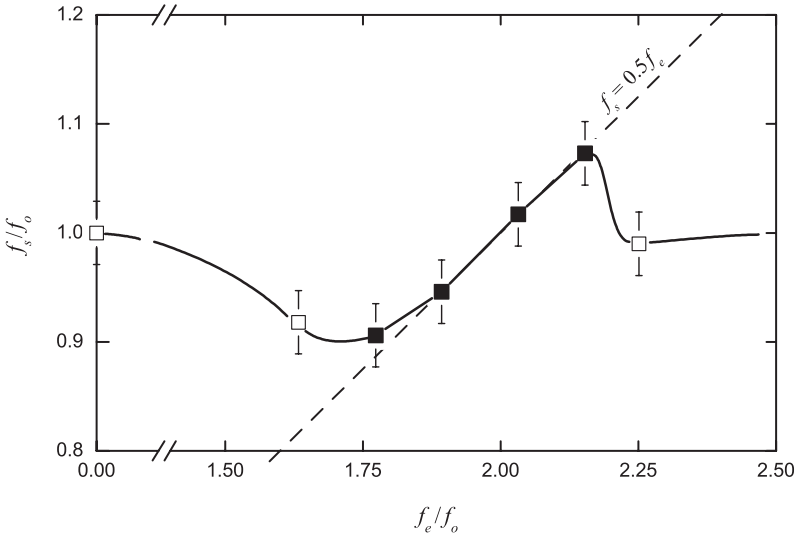

Fig. 8. Variation of the vortex shedding frequency, f_s, as a function of the perturbation frequency, f_e. Values are normalized with the natural shedding frequency ($f_0 = 8.9$ Hz). Solid symbols represent the lock-on state.

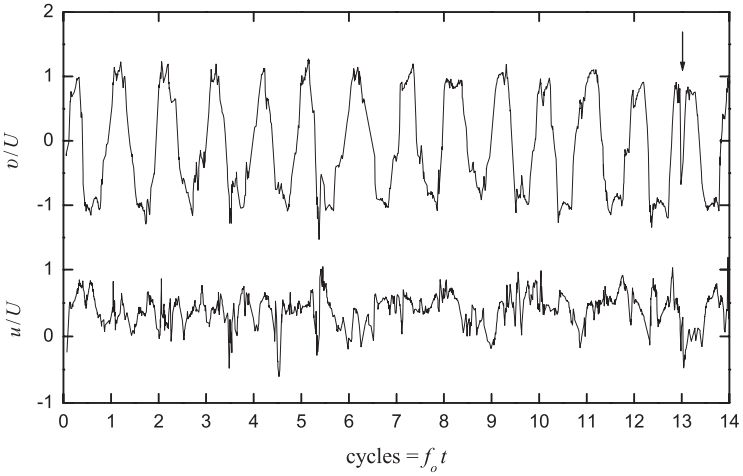

Fig. 9. Instantaneous and simultaneous fluctuations of the streamwise, u, and transverse, v, velocity components at $x/d = 1.75$ in the wake center-line.

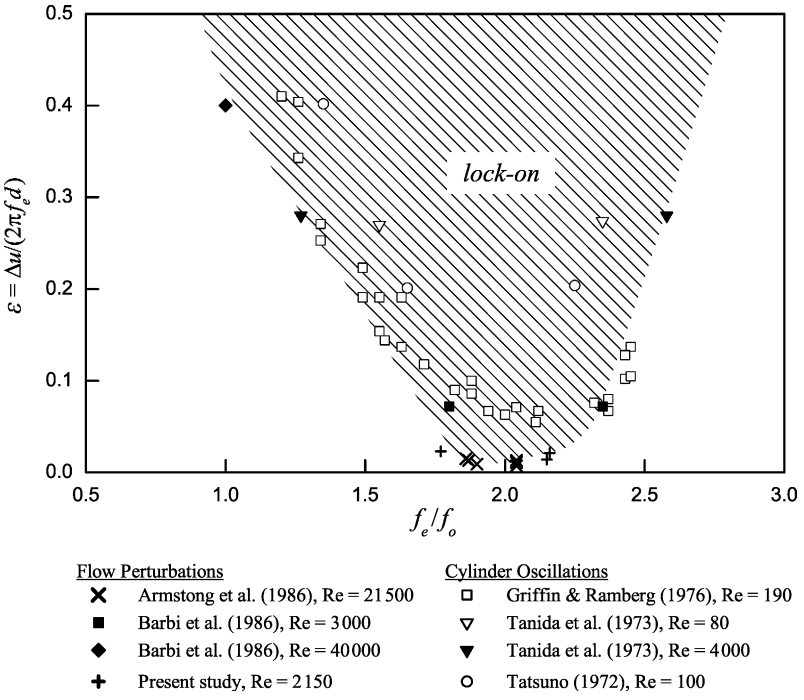

Fig. 10. The limits of the lock-on regime.

amplitude (comparable to the approach flow mean velocity), the streamwise component exhibits random turbulent fluctuations. A change in the phase of the periodic oscillations by π at a particular time can be noted as shown by the arrow in Fig. 9. The behavior of the transverse velocity fluctuations offers a very useful diagnostic tool to assess the state of the wake.

The limits of the lock-on range from previously published data for forced cylinder oscillations or equivalent flow perturbations together with the present data are shown in Fig. 10 in terms of the frequency ratio f_e/f_o and the dimensionless amplitude $\varepsilon = \Delta u/(2\pi f_e d)$, which is equal to the ratio of the amplitude of cylinder oscillation to its diameter or its equivalent for flow perturbations. The data shown indicate the conditions for which lock-on is first observed. The three data-points shown for the present study in Fig. 10 are as follows: two data-points mark the transition between lock-on and no lock-on when the perturbation frequency is varied while the flow velocity and amplitude are maintained constant, and one data-point marks the transition when the amplitude increases while the flow velocity and perturbation frequency are maintained constant. As Barbi et al. (1986) pointed out, there is a dependency of the lock-on limits on the Reynolds number. In order to illustrate this dependency more clearly, data-points representing experiments carried out for $\mathrm{Re} < 350$ are indicated by open symbols and those for $\mathrm{Re} > 350$ by solid symbols in Fig. 10. When this categorization is made, there is good agreement between different experiments and between cylinder oscillations and equivalent flow perturbations. The present data agree well with the published data for high Re and in particular those of Armstrong et al. (1986), despite the fact that the Reynolds numbers in the two experiments are an order of magnitude different. The envelope of the lock-on range is not symmetric with respect to the resonance point, i.e., the range of frequencies for which lock-on occurs is wider for $f_e/f_o < 2$ than for $f_e/f_o > 2$. The threshold amplitude for lock-on to occur is lower at high Re than that at low. The good agreement of the present data with previously published data does not support the expectation that high-turbulence levels might increase the threshold amplitude required to induce lock-on as noted by Blevins (1985). Furthermore, the results suggest that the range of frequency ratios, f_e/f_o, for which lock-on occurs is independent of turbulence intensity, in agreement with published data for sharp-edged bluff bodies (Wolochuk et al., 1996).

4.2. Recirculation bubble and vortex formation region

In this section we examine the effect of flow perturbations on the mean velocity and r.m.s. fluctuations along the center-line of the cylinder wake. From these measurements, the modification of the wake characteristics such as the size

of the recirculation bubble and the vortex formation region was determined. As already mentioned, the experiments were carried out at a constant approach flow velocity of $U = 0.30\,\mathrm{m\,s^{-1}}$ which corresponds to $\mathrm{Re} = 2150$.

The effect of varying the perturbation frequency while the amplitude is kept at a constant value $\Delta u = 0.018\,\mathrm{m\,s^{-1}}$, is examined first. Fig. 11 shows the distribution of the streamwise component of the mean velocity $\bar{u}$ along the wake center-line, normalized with the mean approach velocity U. For clarity, lines are shown which are spline fits to the measured data. The data display a consistent trend: the region of reversed flow (recirculation bubble) reduces in size compared to the unperturbed flow, the extent of the reduction being greater in the middle of the lock-on range. Furthermore, the greater the reduction, the faster (i.e., in shorter length) the recovery of the mean velocity along the wake center-line. Although the distributions show remarkable differences for $x/d < 4$ the mean velocity attains similar values further downstream. This explains the results of Armstrong et al. (1987), who found that the transverse profiles of the mean velocity across the wake center-line at $x/d = 8$ were similar for a perturbed and an unperturbed flow even though the strength of the shed vortices and their arrangement were considerably different. It is the very near wake

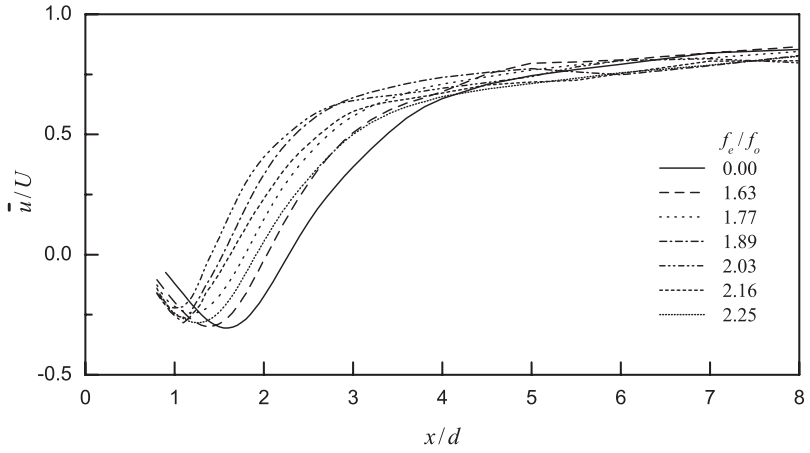

Fig. 11. Distribution of the streamwise mean velocity along the center-line for different values of the perturbation frequency at constant amplitude; $\Delta u/U = 0.06$.

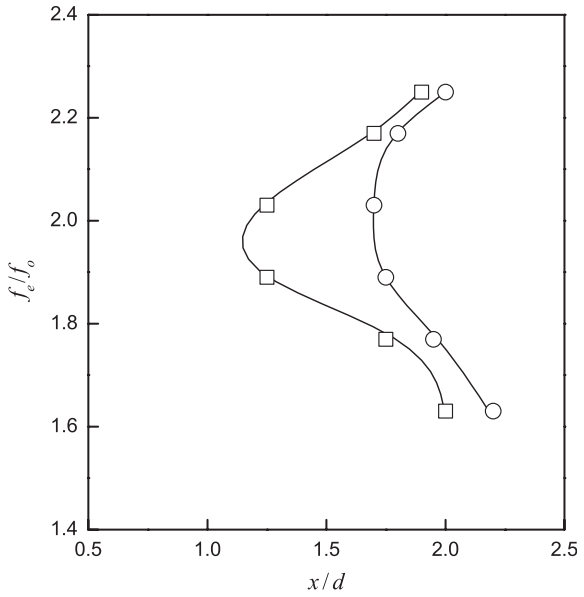

Fig. 12. Variation of the position of the maximum velocity fluctuation along the wake center-line with f_e/f_o:□, $(u'/U)_{\max}$; ○, $(v'/U)_{\max}$.

structure that is modified in order to accommodate the changes in vortex strength, size and trajectory. The maximum velocity deficit varies in a systematic manner and is minimized near the middle of the lock-on range reaching a minimum value of 1.22 compared to 1.30 in the unperturbed flow.

The distributions of the r.m.s. velocities u'/U and v'/U along the wake center-line for the cases of Fig. 11 are not shown here for economy of presentation. These distributions also exhibited a systematic variation with perturbation frequency. Fig. 12 shows the positions of the maximum r.m.s. velocities as a function of the ratio f_e/f_o. The position of the maximum in the streamwise r.m.s. velocity moves from $2.3d$ in the unperturbed flow (not shown on the graph) to $1.25d$ behind the cylinder as the frequency increases to $1.89f_o$, then attains an estimated minimum value of $1.15d$ in the middle of the lock-on range, and then moves back towards its natural position as f_e is increased above $2f_o$. A similar trend is observed for the position of the maximum in the transverse r.m.s. velocity, but the variation is not as pronounced as for the streamwise component.

The above results show that the vortex formation length decreases considerably in the middle of the lock-on range and the roll-up of the shear layers into vortices takes place very close to the back of the cylinder. It might be argued that this modification of the wake structure is associated with the increase in the drag force (or accordingly decrease in the base pressure coefficient) as reported by Tanida et al. (1973) and Armstrong et al. (1986). The minimization of the vortex formation length near the middle of the synchronization range has also been observed for a cylinder forced to oscillate in the transverse direction (Krishnamoorthy et al., 2001). It is very interesting to note that a similar change in the vortex formation length was found in their study (l_f decreased from $2.6d$ for the stationary cylinder to a minimum value of $1.2d$ during lock-on) even though the amplitude was an order of magnitude higher compared to our study ($\varepsilon = 0.22$ compared to approximately 0.02 in the present study). As pointed out by Zdravkovich (1996), the wakes of cylinders forced to oscillate in either the transverse or the streamwise direction share many basic characteristics. However, the present results are in contrast to the reported effects of frequency on the vortex formation length from cylinders oscillating either transversely or in line with the flow direction at Re less than 350 for which frequencies below or above the resonant point ($f_e = f_o$ for transverse and $f_e = 2f_o$ for in-line oscillations) result in an expansion and contraction, respectively, of the formation region compared to the stationary cylinder wake (see Griffin, 1995; Hall and Griffin, 1993; Griffin and Hall, 1991; Griffin and Ramberg, 1976; Griffin and Votaw, 1974).

The maximum intensity of the fluctuations, $(u'/U)_{\max}$ and $(v'/U)_{\max}$ also varies with perturbation frequency. Fig. 13 shows each variation as a function of the vortex formation length l_f/d where each data-point corresponds to a different value of the perturbation frequency as in Fig. 12. Both sets of data exhibit some scatter but clearly $(u'/U)_{\max}$ does not vary appreciably, whereas $(v'/U)_{\max}$ decreases as l_f/d increases. Given the relationship between l_f/d and f_e/f_o shown in Fig. 12, it follows that the intensity of the fluctuations reaches a peak value near the middle of the lock-on range where

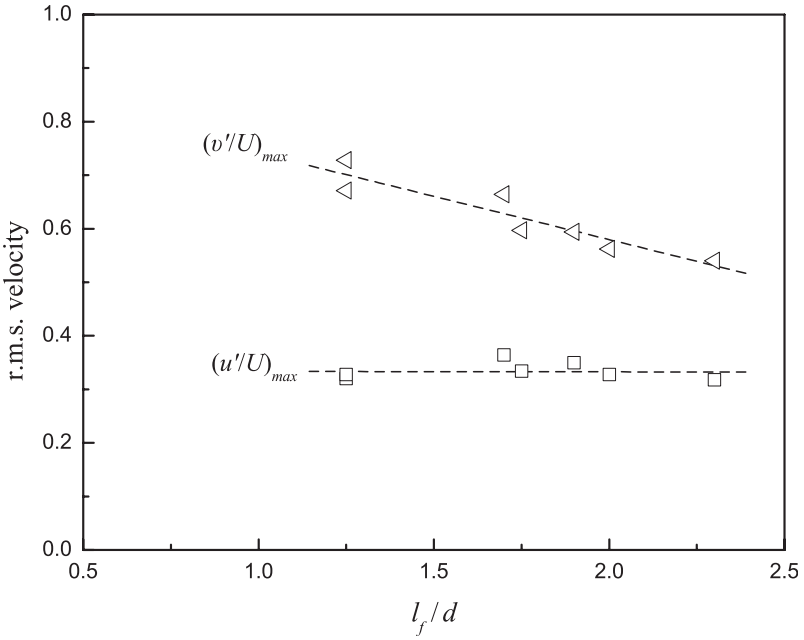

Fig. 13. Variation of the maximum intensity of the velocity fluctuations as a function of the vortex formation length.

the formation length attains its minimum value. This might be expected because the negative base pressure coefficient also attains a peak value near the middle of the lock-on range (Armstrong et al., 1986). One might relate the increased intensity of fluctuations to an increase in the strength of the shed vortices (e.g., see Armstrong et al., 1987), but there is also a dependency on other factors such as the size of the vortices and their arrangement in the vortex street.

The effect of varying the perturbation amplitude on the distributions of the mean velocity and r.m.s. fluctuation along the wake center-line, is examined next. The perturbation frequency was held constant at $f_e/f_o = 1.86$ and 2.15. The experiments were carried out at a constant approach flow velocity of $0.30\,\mathrm{m\,s^{-1}}$ ($\mathrm{Re} = 2150$), which is the same as in the experiments with varying perturbation frequency. Fig. 14 shows the distribution of the streamwise mean velocity $\bar{u}/U$ along the wake center-line for different amplitudes of flow perturbation. Increasing the amplitude results in a monotonic reduction of the recirculation bubble length and a faster recovery of the mean velocity deficit. However, for $x/d > 4$ the mean velocity does not change appreciably. Govardhan and Williamson (2001) have also observed the shortening of the recirculation bubble up to its complete elimination with increased amplitude of oscillation for an elastically mounted cylinder oscillating freely in the transverse direction.

Fig. 15 shows the variation in the positions of $(u'/U)_{\max}$ (vortex formation length) and $(v'/U)_{\max}$ with perturbation amplitude. Both the above positions move upstream with increasing amplitude in a similar fashion. The position of

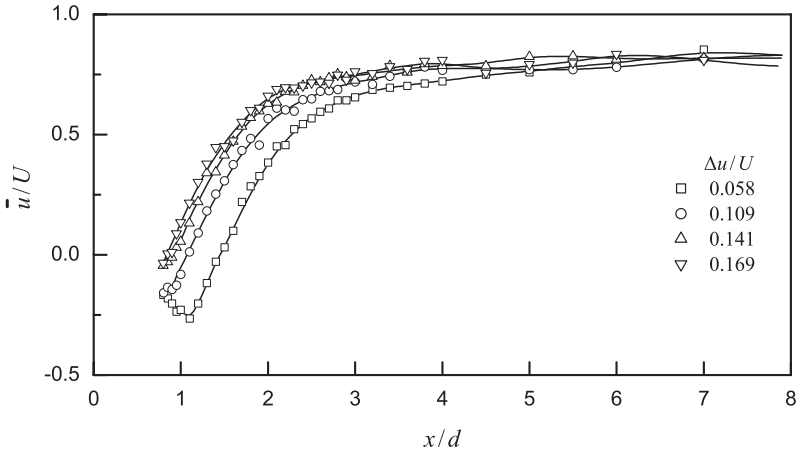

Fig. 14. Distribution of the streamwise mean velocity along the center-line for different values of the perturbation amplitude at constant frequency; $f_e/f_o = 1.86$.

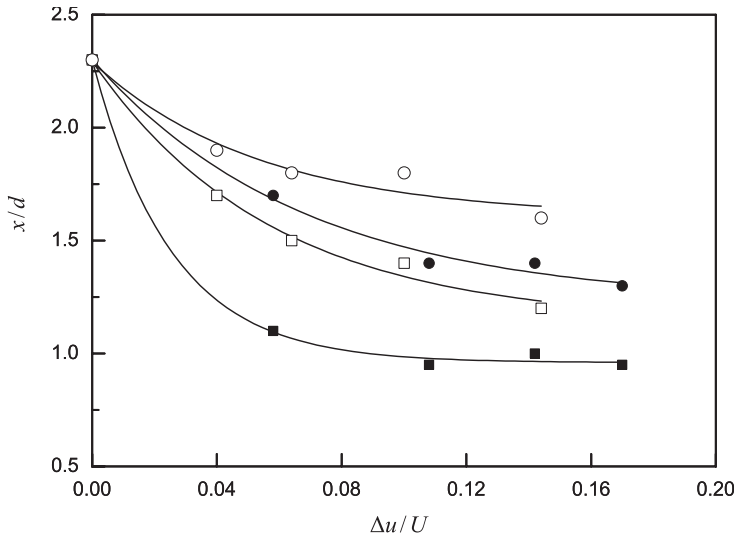

Fig. 15. Variation of the position of the maximum velocity fluctuation along the wake centerline with $\Delta u/U$. $f_e/f_o = 1.86$: ■, $(u'/U)_{\max}$, ●, $(v'/U)_{\max}$; $f_e/f_o = 2.15$: □, $(u'/U)_{\max}$, ○, $(v'/U)_{\max}$.

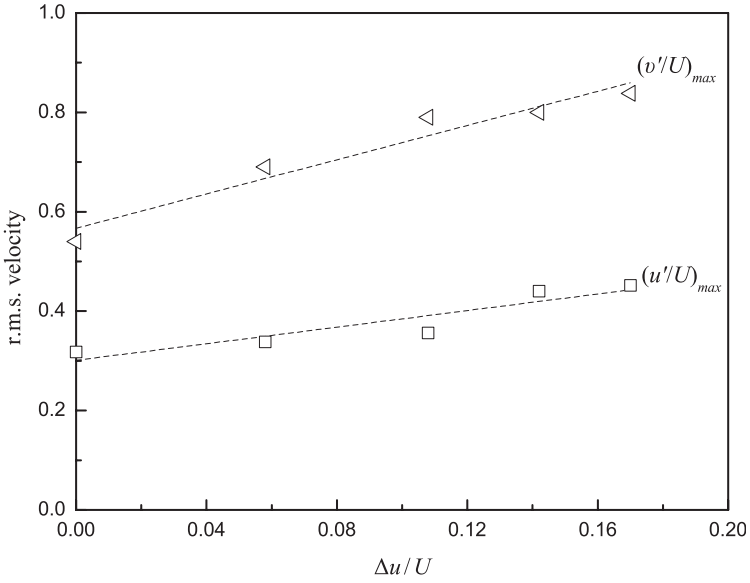

Fig. 16. Variation of the maximum intensity of the velocity fluctuations as a function of the perturbation amplitude.

$(v'/U)_{\max}$ lies always downstream of that of $(u'/U)_{\max}$ as in the unperturbed flow. The data for $f_e/f_o = 1.86$ suggest a limiting vortex formation length of about one diameter. Not only the position but also the magnitude of the maximum r.m.s. values of the velocity fluctuations in the wake center-line change with the perturbation amplitude as shown in Fig. 16. Both $(u'/U)_{\max}$ and $(v'/U)_{\max}$ values increase with increasing amplitude. Again, this effect might be associated with a more negative base pressure coefficient and a selective increase in vortex strength but other factors might contribute as well. One such factor is the orientation of the vortex filaments relative to the cylinder axis. Two-point LDA measurements just outside the separating shear layer showed that the correlation of the velocity fluctuations along the cylinder span increases with increasing perturbation amplitude. It might be expected that, at lock-on, nearly parallel vortex shedding occurs over the central part of the span where the measurements were made. This would lead to an apparent increase in vortex strength measured in a slice of the flow perpendicular to the cylinder axis. Griffin and Ramberg (1976) have also noted that the flow becomes more '2-D' at lock-on.

It is also interesting to look at the relationship between the recirculation bubble length and the formation length, shown in Fig. 17. Error bars indicate the experimental uncertainty in determining the two length scales. There is a nearly linear relationship between these two length scales. In general, the end of the formation region coincides with the end of the recirculation bubble within the experimental error. However, at high perturbation amplitudes for which more complex vortex patterns might occur, this relationship may break down.

4.3. Longitudinal vortex spacing

The relative phase difference between the velocity fluctuations in the wake and the approach flow perturbations was estimated from the time-resolved LDA data in order to determine the effects of frequency and amplitude on the wavelength of the vortex street (longitudinal vortex spacing). The transverse velocity fluctuations which exhibited well-defined large-amplitude oscillations were used for the analysis.

Fig. 18 shows the time history of the fluctuating low-pass filtered velocity signal at a point in the wake and the arrival time of the reference pulses from the shaft encoder, which was attached to the rotating valve that generated the flow perturbations. The methodology is only correct for conditions of vortex shedding lock-on under which there is a correlation between the wake velocity fluctuations and the imposed perturbations as in Fig. 18. The methodology is analogous to that used by Griffin and co-workers to determine the vortex spacing behind oscillating cylinders (Griffin and Votaw, 1974; Griffin and Ramberg, 1976).

Fig. 19 shows the relative phase difference, ϕ, as a function of the normalized downstream distance, $(x/d)(f_e/2f_o)$, when the perturbation frequency is varied while the perturbation amplitude is maintained constant whereas, in Fig. 20, the amplitude is varied and the frequency is maintained constant. The phase difference has been adjusted (a constant value was subtracted) so that $\phi = 0^\circ$ at $x/d = 0$. Close to the cylinder base, the relative phase difference is not

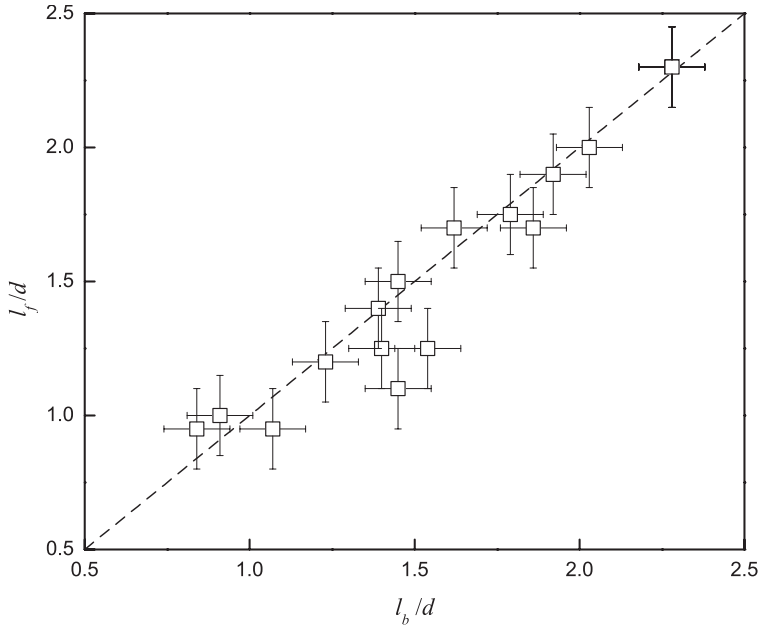

Fig. 17. Relationship between the recirculation bubble length l_b and the vortex formation length l_f.

representative of the vortex spacing and data in this region is not included. Further downstream, the relative phase difference varies linearly with distance and the longitudinal vortex spacing, λ, may be estimated from

$$\frac{\lambda}{d}\left(\frac{f_e}{2f_o}\right) = 360\,\frac{\Delta[(x/d)(f_e/2f_o)]}{\Delta\phi}, \tag{3}$$

which can be determined from a least-squares linear fit to the data. The vortex spacing results are summarized in Table 3. In the unperturbed flow, the vortex spacing was estimated from the relative phase difference between two fluctuating velocity signals using two measuring LDA probes, one located downstream of the other and separated by one diameter; the upstream probe was located at $(x/d, y/d) = (3, 1)$. However, because the value obtained is, firstly, based on a single measurement and, secondly, it is known that this value depends on x/d as well as y/d (Simmons, 1974), the result should be treated cautiously. Nonetheless, the obtained longitudinal vortex spacing of $4.5d$ compares well with the value of $4.6d$ found by Armstrong et al. (1987).

The results in Table 3 suggest an inverse relationship between λ and f_e; perturbation frequencies above twice the natural Strouhal frequency result in a decrease in the longitudinal vortex spacing from that in the unperturbed flow and vice versa. This finding agrees well with the results obtained in the wake of cylinders oscillating either transversely or in line with the flow direction (Griffin and Votaw, 1974; Griffin and Ramberg, 1976). However, no systematic trend is observed when the perturbation amplitude is increased. Griffin and Ramberg (1976) found that increasing the amplitude of in-line cylinder oscillations decreases the transverse spacing of the vortices in the Kármán vortex street resulting in a nearly collinear array of vortices at sufficiently high amplitude but did not alter the longitudinal vortex spacing. Therefore, it might be reasonable to assume that, also in the present case, there is no change in the longitudinal vortex spacing with perturbation amplitude and that the variability of the vortex spacing results is due to the uncertainty of the methodology used. It should be noted that, in the present study, the perturbation amplitude is relatively small and the wake is turbulent and, as a result, the lock-on signature is not very pronounced.

The variation of the longitudinal vortex spacing as a function of the frequency ratio, $f_e/2f_o$, within the lock-on range for streamwise cylinder oscillations and equivalent flow perturbations is shown in Fig. 21. The ordinate is the dimensionless vortex spacing multiplied by the unforced Strouhal number. The Strouhal number values for the experiments of Tatsuno (1972) at $\mathrm{Re} = 100$ and Griffin and Ramberg at $\mathrm{Re} = 190$ were estimated using

$$\mathrm{St} = a\mathrm{Re} + b/\sqrt{\mathrm{Re}} + c/\mathrm{Re}, \tag{4}$$

with $a = 0.2850$, $b = -1.3897$ and $c = 1.8061$ given by Williamson and Brown (1998) to represent the Strouhal–Reynolds number relationship for '2-D' vortex shedding in the laminar regime. Despite the fact that the experiments encompass a range of Reynolds numbers from 100 to 21500 and different methods to achieve vortex shedding lock-on,

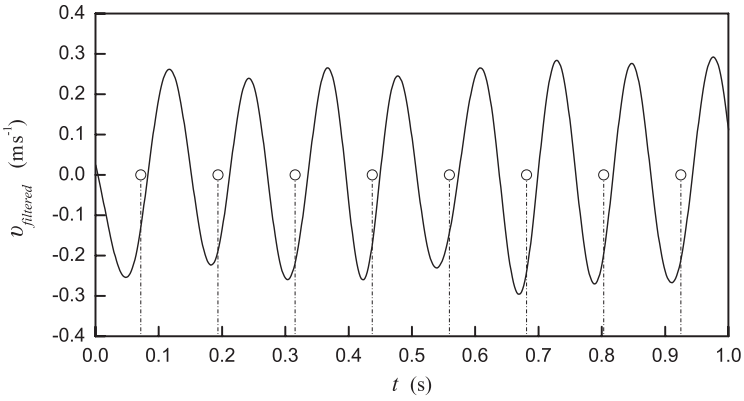

Fig. 18. Fluctuating velocity signal and arrival time of the reference pulses from the shaft encoder.

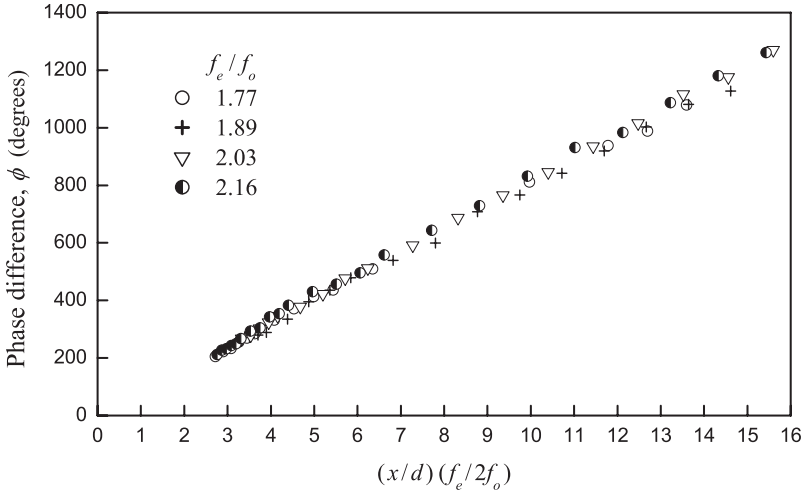

Fig. 19. Relative phase difference, ϕ, as a function of the normalized distance $(x/d)(f_e/2f_o)$ for different frequencies at constant amplitude.

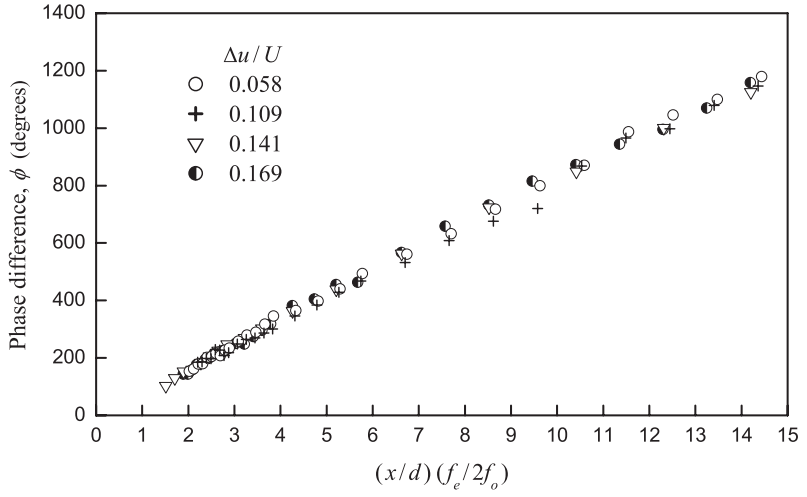

Fig. 20. Relative phase difference, ϕ, as a function of the normalized distance $(x/d)(f_e/2f_o)$ for different frequencies at constant frequency.

Table 3
Longitudinal vortex spacing behind a circular cylinder in perturbed flow, Re = 2150

Frequency ratio, f_e/f_o	Amplitude ratio, $\Delta u/U$	Vortex spacing, λ/d	$(\lambda/d)(f_e/2f_o)$
0.00	0.00	4.5[a]	—
1.77	0.06	5.0	4.4
1.89	0.06	4.7	4.4
2.03	0.06	4.3	4.4
2.16	0.06	4.0	4.3
1.86	0.06	4.6	4.3
1.86	0.11	4.4	4.1
1.86	0.14	4.6	4.3
1.86	0.17	4.8	4.5
2.15	0.04	4.0	4.3
2.15	0.06	4.1	4.3
2.15	0.10	4.0	4.3
2.15	0.14	3.9	4.3

[a] Measured with two probes.

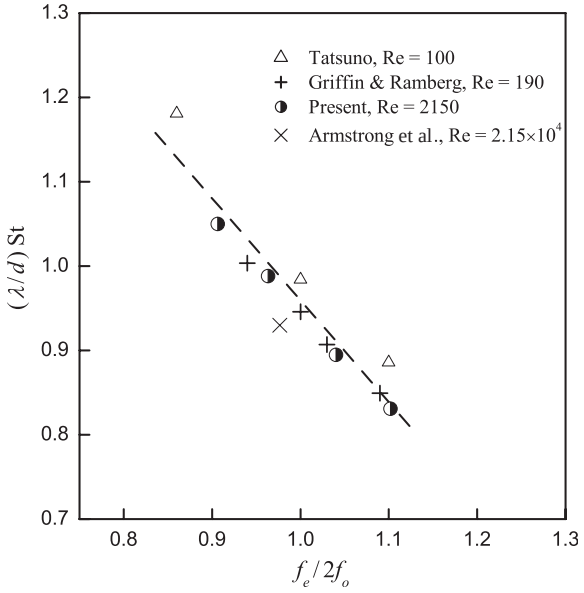

Fig. 21. Longitudinal vortex spacing $(\lambda/d)\,\mathrm{St}$ as a function of frequency ratio $f_e/2f_o$.

the data in Fig. 21 fit well together and follow an inverse linear relationship, which is represented by the following straight line obtained with a least-squares fit,

$$\frac{\lambda}{d}\,\mathrm{St} = (2.17 \pm 0.11) - (1.21 \pm 0.11)\left(\frac{f_e}{2f_o}\right). \tag{5}$$

The vortex convection speed, C_v, can be estimated from the longitudinal vortex spacing and the vortex shedding frequency using

$$\frac{C_v}{U} = \frac{\lambda f_s}{U} = \frac{\lambda}{d}\left(\frac{f_e}{2f_o}\right)\mathrm{St}, \tag{6}$$

since $f_e/f_o = 2$ at lock-on. Using all the experimental data shown in Fig. 21, it is found that the vortex convection speed has a nearly constant value of $C_v/U = 0.95 \pm 0.03$. Although this value is slightly higher than the value of 0.93 reported by Hall and Griffin (1993), the constant convection speed is representative of a nondispersive physical system. Griffin

and Hall (1991) showed that both unforced and forced vortex wakes generated by bluff bodies with different geometries share the same nondispersive character over a wide range of Re.

5. Conclusions

An experimental study of the wake of a circular cylinder in steady (unperturbed) and perturbed approach flows was conducted in a water tunnel. The velocity fluctuations of the streamwise and transverse components were measured along the wake center-line with a laser-Doppler anemometer. The main conclusions from this study are summarized below.

The length of the recirculation bubble and the vortex formation region decrease abruptly as the Reynolds number increases between 1750 and 10^4 in steady (unperturbed) flow. Even though, this large decrease has been consistently observed in previous studies (e.g., see Unal and Rockwell, 1988; Lin et al., 1995), it might be argued that the relatively high-turbulence level and high tunnel blockage in the present experiments raises the effective Re of the flow and results in a more pronounced decrease compared to low-turbulence, low-blockage experiments. This is particularly true for the recirculation bubble length whereas the vortex formation length appears less sensitive to the above influencing parameters. An interlinked effect is that the magnitude of the velocity fluctuations in the near wake, particularly the component across the center-line, increases in this Re range.

The main focus of this study is on the effect of velocity perturbations superimposed on the mean approach flow on the wake characteristics. The lock-on phenomenon, where the vortex shedding frequency is captured by the perturbation frequency, was observed in agreement with previous experimental studies of either perturbed flows around stationary cylinders or the equivalent case of cylinders oscillating in line with the incident steady flow, when the perturbation frequency takes values around twice the natural Strouhal frequency. As the perturbation frequency is varied so that the limits of the lock-on range are crossed, the recirculation bubble and the vortex formation region shrink systematically in size and attain minimum values near the middle of the lock-on range, i.e., close to the resonance point $f_e/f_o = 2$. The effect of increasing the perturbation amplitude at a constant frequency results in a further reduction of the extent of the recirculation bubble and the vortex formation region. Generally, the positions that mark the end of these two characteristic regions occur close together and vary in a similar manner with frequency and amplitude.

The maximum intensity of the velocity fluctuations along the center-line of the cylinder wake increases for both the streamwise and particularly the transverse component as the vortex formation length decreases. This suggests that the closer the vortices form to the cylinder base, the stronger they are. The intensification of the velocity fluctuations in the near wake near the middle of the lock-on range might be associated with the more negative base pressure coefficient found in relevant studies (Armstrong et al., 1986; Barbi et al., 1986).

The wavelength of the vortex street varies inversely with the perturbation frequency; frequencies above and below two times the natural Strouhal frequency decrease and increase, respectively, the longitudinal vortex spacing compared to that in the unperturbed flow in analogy to the effects reported for oscillating cylinders. The amplitude of the perturbations does not appear to alter the vortex spacing.

Strictly speaking, the results obtained in this study are only applicable for the particular experimental configuration employed. The cylinder aspect ratio, the turbulence level of the approach flow, the tunnel blockage and the proximity of the test-section walls are all expected to have an effect on the results. However, the present results give a good comparison with previous results from other authors, particularly at $\mathrm{Re} = 2150$ employed for the perturbed flow experiments. Furthermore, the perturbations increase the spanwise correlation of the flow and, hence, lessen the influence of three-dimensional effects on the results. Similar variations in the wake characteristics due to flow perturbations as those found in the present study are therefore to be expected for infinitely long cylinders in unconfined smooth flows.

The effects of flow perturbations in terms of frequency and amplitude on the wake characteristics reported here exhibit remarkable similarity with the forced wakes from cylinders oscillating in either the streamwise or transverse direction at relatively high Reynolds numbers (greater than 350). An important finding of this study is that relatively low-amplitude flow perturbations can cause a strong modification of the wake structure comparable to that of cylinders oscillating at high amplitude. For the relatively low amplitudes employed in the present study, the wake pattern probably does not change and remains at the 2-S mode of Williamson and Roshko (1988) where two single vortices are shed antisymmetrically during each cycle. However, higher amplitudes can introduce strong nonlinearities and complex changes in the wake pattern, for example, see the visualization photographs of Griffin and Ramberg (1976). A related phenomenon is the formation of symmetric 'twin' vortices in the near wake synchronized with the cylinder oscillation or flow perturbation as observed by Barbi et al. (1986) and Ongoren and Rockwell (1988). The former authors observed

the symmetric mode for frequencies around $f_e/f_o = 1$ whereas the latter around $f_e/f_o = 3$, but the effect of amplitude was not examined in both studies. The flow conditions for which symmetric vortex formation occurs are not known as yet and further experiments are required to clarify this issue.

Acknowledgements

The authors gratefully acknowledge financial support received by the Engineering and Physical Sciences Research Council of the United Kingdom through Grant GR/R29802/01.

References

Armstrong, B.J., Barnes, F.H., Grant, I., 1986. The effect of a perturbation on the flow over a bluff cylinder. Physics of Fluids 29, 2095–2102.

Armstrong, B.J., Barnes, F.H., Grant, I., 1987. A comparison of the structure of the wake behind a circular cylinder in steady flow with that in a perturbed flow. Physics of Fluids 30, 19–26.

Barbi, C., Favier, D.P., Maresca, C.A., Telionis, D.P., 1986. Vortex shedding and lock-on of a circular cylinder in oscillatory flow. Journal of Fluid Mechanics 170, 527–544.

Bearman, P.W., 1984. Vortex shedding from oscillating bluff bodies. Annual Review of Fluid Mechanics 16, 195–222.

Blevins, R.D., 1985. The effect of sound on vortex shedding from cylinders. Journal of Fluid Mechanics 161, 217–237.

Bloor, M.S., 1964. The transition to turbulence in the wake of a circular cylinder. Journal of Fluid Mechanics 19, 290–303.

Bloor, M.S., Gerrard, J.H., 1966. Measurements of turbulent vortices in a cylinder wake. Proceedings of the Royal Society of London Series A 294, 319–342.

Buchhave, P., George, W.K., Lumley, J.L., 1979. The measurement of turbulence with the laser-Doppler anemometer. Annual Review of Fluid Mechanics 11, 443–503.

Cantwell, B., Coles, D., 1986. An experimental study of entrainment and transport in the turbulent near wake of a circular cylinder. Journal of Fluid Mechanics 136, 321–374.

Carberry, J., Sheridan, J., Rockwell, D., 2001. Forces and wake modes of an oscillating cylinder. Journal of Fluids and Structures 15, 523–532.

Durst, F., Jovanović, J., Sender, J., 1995. LDA measurements in the near-wall region of a turbulent pipe flow. Journal of Fluid Mechanics 295, 305–335.

Durst, F., Melling, A., Whitelaw, J.H., 1976. Principles and Practices of Laser Doppler Anemometry. Academic Press, New York.

Gerrard, J.H., 1966. The mechanics of the formation region of the vortices behind bluff bodies. Journal of Fluid Mechanics 25, 401–413.

Govardhan, R., Williamson, C.H.K., 2001. Mean and fluctuating velocity fields in the wake of a freely vibrating cylinder. Journal of Fluids and Structures 15, 489–501.

Green, R.B., Gerrard, J.H., 1993. Vorticity measurements in the near wake of a circular cylinder at low Reynolds numbers. Journal of Fluid Mechanics 246, 675–691.

Griffin, O.M., 1995. A note on bluff body vortex formation. Journal of Fluid Mechanics 284, 217–224.

Griffin, O.M., Hall, M.S., 1991. Vortex shedding lock-on and flow control in bluff body wakes—review. ASME Journal of Fluids Engineering 113, 526–544.

Griffin, O.M., Ramberg, S.E., 1976. Vortex shedding from a cylinder vibrating in line with an incident uniform flow. Journal of Fluid Mechanics 75, 526–537.

Griffin, O.M., Votaw, C.M., 1974. The vortex street in the wake of a vibrating cylinder. Journal of Fluid Mechanics 51, 31–48.

Hall, S.E., Griffin, O.M., 1993. Vortex shedding and lock-on in a perturbed flow. ASME Journal of Fluids Engineering 115, 283–291.

Konstantinidis, E., 2001. Pulsating flow in cylinder arrays. Ph.D. Thesis, King's College London, University of London.

Krishnamoorthy, S., Price, S.J., Païdoussis, M.P., 2001. Cross-flow past an oscillating circular cylinder: synchronization phenomena in the near wake. Journal of Fluids and Structures 15, 955–980.

Lin, J.C., Towfighi, F., Rockwell, D., 1995. Instantaneous flow structure on the near wake of a circular cylinder: on the effect of Reynolds number. Journal of Fluids and Structures 9, 409–418.

Ma, X., Karamanos, G.S., Karniadakis, G.E., 2000. Dynamics and low-dimensionality of a turbulent near wake. Journal of Fluid Mechanics 410, 29–65.

McKillop, A.A., Durst, F., 1984. LDA experiments of separated flow behind a circular cylinder. Second International Symposium of Laser Doppler Anemometry Applications to Fluid Mechanics, paper 14.4.

Norberg, C., 1986. Interaction of free stream turbulence and vortex shedding for a single tube in cross-flow. Journal of Wind Engineering and Industrial Aerodynamics 23, 501–514.

Ongoren, A., Rockwell, D., 1988. Flow structure from an oscillating cylinder. Part 2. Mode competition in the near wake. Journal of Fluid Mechanics 191, 225–245.

Sarpkaya, T., 1979. Vortex induced oscillations. Journal of Applied Mechanics 46, 241–258.

Simmons, E.L., 1974. Phase-angle measurements between two hot-wire signals in the turbulent wake of a two-dimensional bluff body. Journal of Fluid Mechanics 64, 599–609.

Tanida, Y., Okajima, A., Watanabe, Y., 1973. Stability of a circular cylinder oscillating in uniform flow or in a wake. Journal of Fluid Mechanics 61, 769–784.

Tatsuno, M., 1972. Vortex streets behind a circular cylinder oscillating in the direction of flow. Bulletin of the Research Institute for Applied Mechanics of Kyushu University 36, 25–37.

Unal, M.F., Rockwell, D., 1988. On vortex formation from a cylinder. Part 1. The initial instability. Journal of Fluid Mechanics 190, 491–512.

Williamson, C.H.K., Brown, G.L., 1998. A series in $1/\sqrt{\mathrm{Re}}$ to represent the Strouhal–Reynolds number relationship of the cylinder wake. Journal of Fluids and Structures 12, 1073–1085.

Williamson, C.H.K., Roshko, A., 1988. Vortex formation in the wake of an oscillating cylinder. Journal of Fluids and Structures 2, 355–381.

Wolochuk, M.C., Plesniak, M.W., Braun, J.E., 1996. The effects of turbulence and unsteadiness on vortex shedding from sharp-edged bluff bodies. ASME Journal of Fluids Engineering 118, 18–25.

Zdravkovich, M.M., 1996. Different modes of vortex shedding: an overview. Journal of Fluids and Structures 10, 427–437.

Zdravkovich, M.M., 1997. Flow around Circular Cylinders. Oxford University Press, Oxford.